Photocatalysis

How to cite: *Angew. Chem. Int. Ed.* **2023**, *62*, e202219086
International Edition: doi.org/10.1002/anie.202219086
German Edition: doi.org/10.1002/ange.202219086

Copper(I) Photocatalyzed Bromonitroalkylation of Olefins: Evidence for Highly Efficient Inner-Sphere Pathways

Alexander Reichle[+], Magdalena Koch[+], Hannes Sterzel, Lea-Joy Großkopf, Johannes Floss, Julia Rehbein, and Oliver Reiser**

Abstract: We report the visible light-mediated copper-catalyzed vicinal difunctionalization of olefins utilizing bromonitroalkanes as ATRA reagents. This protocol is characterized by high yields and fast reaction times under environmentally benign reaction conditions with exceptional scope, allowing the rapid functionalization of both activated and unactivated olefins. Moreover, late-stage functionnalization of biologically active molecules and upscaling to gram quantities is demonstrated, which offers manifold possibilities for further transformations, e.g. access to nitro- and aminocyclopropanes. Besides the synthetic utility of the title transformation, this study undergirds the exclusive role of copper in photoredox catalysis showing its ability to stabilize and interact with radical intermediates in its coordination sphere. EPR studies suggest that such interactions can even outperform a highly favorable cyclization of transient to persistent radicals contrasting iridium-based photocatalysts.

ATRA (atom transfer radical addition) reactions are a powerful tool to construct molecules in an atom- and step-economic fashion, reaching back to the 1940s with the pioneering work of Kharasch.[1] In combination with visible-light photoredox catalysis[2] ATRA reactions could be developed in great variety,[3] allowing the addition of suitable precursors RX across the double bond of alkenes (Scheme 1). Cu^{I}-phenanthroline complexes, in particular $[Cu^{I}(dap)_2]Cl$ (dap = 2,9-bis(*para*-anisyl)-1,10-phenanthroline) as a stand-alone photocatalyst or iridium-based photocatalysts in combination with Cu^{II}-additives[4] are especially effective for this transformation, which is attributed to the ability of Cu^{II}, being a persistent radical, to interact with a transient radical to ultimately deliver X^- via a Cu^{III}-intermediate (Scheme 1).

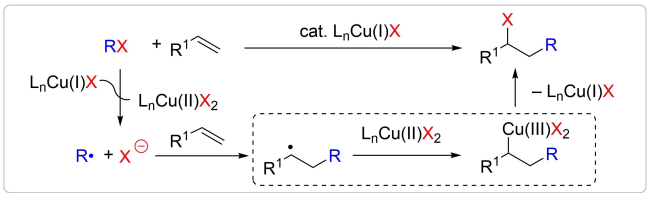

Scheme 1. Cu^{I} photocatalyzed ATRA reactions.

As a consequence of such an inner-sphere mode, a number of ATRA processes have been reported that are not possible with other photoredox catalysts, e.g. with those based on ruthenium, iridium, or organic dyes.[5] To date, only few ATRA and related transformations between organobromonitroalkanes have been reported.[6,7] We were intrigued by the report by Ooi and co-workers,[7] who demonstrated the iridium(III)-catalyzed, photodivergent addition of bromonitroalkanes **1** to styrenes **2** (Scheme 2).

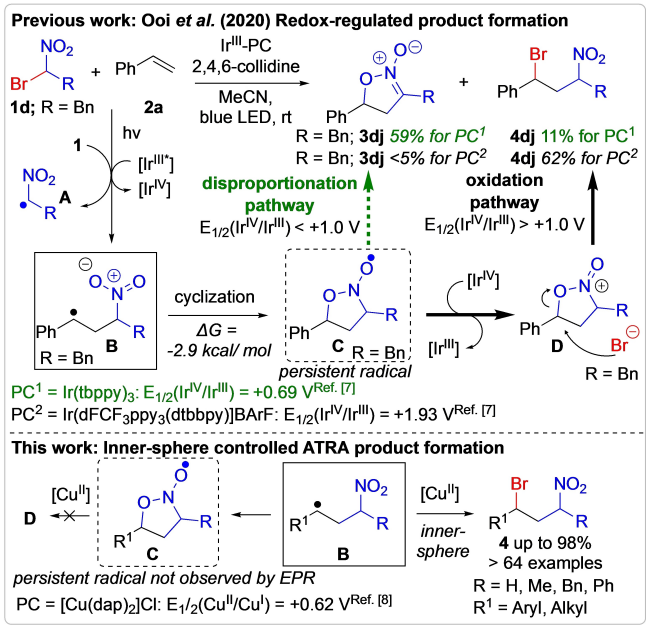

Scheme 2. Divergent pathways in ATRA reactions between bromonitroalkanes and alkenes.

[*] A. Reichle,[+] M. Koch,[+] H. Sterzel, L.-J. Großkopf, J. Floss, Prof. Dr. J. Rehbein, Prof. Dr. O. Reiser
Fakultät Chemie & Pharmazie, Universität Regensburg
Universitätsstr. 31, 93053 Regensburg (Germany)
E-mail: Julia.Rehbein@chemie.uni-regensburg.de
olver.reiser@chemie.uni-regensburg.de
Homepage: http://www-oc.chemie.uni-regensburg.de/reiser/index_e.html

[+] co-first authors

As the key intermediate, the persistent radical **C** was proposed based on DFT calculations, rapidly forming via the cyclization of **B**. It was shown that if the oxidized photocatalysts cannot oxidize **C** (i.e. $E_{1/2}(Ir^{IV}/Ir^{III} < 1.0$ V), the isoxazoline-*N*-oxide **3** is formed as the major product via a disproportionation pathway. On the other hand, for iridium photocatalysts with $E_{1/2}(Ir^{IV}/Ir^{III} > 1.0$ V), the ATRA product **4** is obtained as the major product via oxidation of **C** to **D**. Based on this analysis, we expected that copper(II), e.g. in $[Cu(dap)_2]Cl$[8a] $E_{1/2}(Cu^{II}/Cu^{I} = 0.62$ V vs. saturated calomel electrode (SCE)) having lower oxidizing power such as $[Ir(tbppy)_3]^+$ $E_{1/2}(Ir^{IV}/Ir^{III} = 0.69$ V vs. SCE)[7] or $[Ir(ppy)_3]$ $E_{1/2}(Ir^{IV}/Ir^{III} = 0.77$ V vs. SCE)[8b] should also result in **3** unless Cu^{II} could successfully compete with the cyclization to **C**. Indeed, Iwasaki et al. already had shown that the related thermal reaction between **1e** (R = Ph) and **2a** initiated by $Cu(OH)_2$ (50 mol %) exclusively leads to isoxazoline-*N*-oxide of type **3** in 84 % yield.[6c]

We started our investigation by irradiating bromonitromethane[9] (**1a**) and styrene (**2a**) in the presence of $[Cu^{I}(dap)_2]Cl$ with a blue or green LED (455 or 530 nm, Table 1, entries 1–2). The ATRA product **4a** was exclusively obtained in 87–90 % yield. $[Cu^{II}(dap)Cl_2]$, which is readily reduced under photochemical conditions to $Cu^{I}(dap)Cl$ by homolysis of the Cu–Cl bond,[10] can be successfully employed with similar results (entry 3). The addition of collidine, which was found to be beneficial in the iridium-catalyzed processes to form either **3** or **4**,[7] somewhat slowed down the copper-catalyzed process but gave rise to **4a** in good yield (entry 4). Other Cu^{I} complexes being also established as photocatalysts such as $[Cu^{I}(dmp)_2]Cl$[8] (dmp = 2,9-dimethyl1,10-phenanthroline) or $[Cu^{I}(Xanthphos)(dmp)]BF_4$[11] (Xantphos = 4,5-bis(diphenylphosphino)-9,9-dimethylxanthene) were found to promote the desired transformation as well, but with slightly reduced efficiency (entries 5–6). Performing the reaction without a photocatalyst or light gave no desired product (entries 7–8). The use of copper(I)- or copper(II)-chloride or the attempt to start a radical chain process with AIBN under thermal conditions does not promote the reaction either (entries 9–10). In line with the observation of Ooi and co-workers,[7] non-copper-based metal- or organo-photocatalyst would only give rise to **4a** if the oxidized photocatalyst would be a strong oxidant. However, none could rival the efficiency of the copper catalysts for the title transformation (for details, see the Supporting Information).

Table 1: Reaction Optimization.[a]

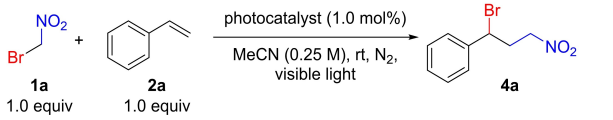

Entry	Catalyst	LED [nm]	Time [h]	Yield[b] [%]
1	$[Cu^{I}(dap)_2]Cl$	530	1	87
2	$[Cu^{I}(dap)_2]Cl$	455	1	90
3	$[Cu^{II}(dap)Cl_2]$	530	2	87
4	$[Cu^{I}(dap)_2]Cl$/collidine (1 equiv)	455	2	66
5	$[Cu^{I}(dmp)_2]Cl$	455	2	80
6	$[Cu^{I}(Xanthphos)(dmp)]BF_4$	455	3	83
7	no	455	1	nr
8	$[Cu^{I}(dap)_2]Cl$ or $[Cu^{I}(dap)Cl_2]$	no	2	nr
9	$Cu^{I}Cl$ or $Cu^{II}Cl_2$ (10 mol %)	455	3	nr
10	AIBN (10 mol %), 80 °C	no	1	nr

Reaction conditions: [a] styrene (**2a**, 0.25 mmol), bromonitromethane (**1a**, 0.25 mmol), and catalyst (2.5 μmol, 1.0 mol %) in MeCN (1.0 mL, 0.25 M). [b] ^{1}H NMR yield using 1,1,2,2-tetrachloroethane as an internal standard. nr = no reaction.

We next explored the type of alkenes that can be employed for the title reaction under Cu^{I}-photocatalysis, revealing an exceptional scope much broader than for most other ATRA reactions[3] (Scheme 3). Starting with activated olefins, styrenes containing weak electron-donating alkyl substituents at the ortho, meta, or para position resulted in the desired products **4b–4e, 4g–j**. A further increase of the electron-donating character in the styrene (*p*-OMe), however, gave a complex reaction mixture, which is in agreement with previous studies on Cu^{I}-catalyzed ATRA reactions.[12] When the methoxy group is located in meta position, acting this way as an acceptor, **4g** was obtained in 74 % yield. While α-substitution on the styrene moiety led to a complex reaction mixture, β-substitution was tolerated well (**4m**). A benzyl-chloride-containing styrene that could have undergone a photoreduction to form a benzyl radical[13] was nevertheless selectively converted to **4n**. Investigating *N*-heterocycles, 2-vinyl pyridine delivered the corresponding product **4p**, however, when the vinyl-moiety was placed in *p*-position, a complex reaction mixture was observed. Electron-withdrawing halogen substitutions in different positions and *p*-CF_3, *p*-CN, or *p*-NO_2 were tolerated well and yielded products **4r–4ab** in high yields. A limitation regarding the protocol was observed for alkynes: A complex reaction mixture for **4ac** or no conversion in the case of **4ad** was observed. 1,3-dienes give rise to a 1,4-radical addition (**4ae**). The protocol was also suitable to convert α,β-unsaturated Michael systems, usually challenging for the addition of electrophilic radicals,[12,14] in moderate to good yields (**4ba**, **4bb**, Scheme 3B). Unactivated alkenes proved to be suitable substrates for this reaction (Scheme 3C), tolerating a variety of functional groups such as trimethylsilyl (**4cc**), halides (**4cd**, **4ce**), cyano (**4cf**), aldehyde (**4ci**) or epoxide (**4cj**) substituents (Scheme 3C). Employing alkyl-substituted bromonitroalkanes was possible, giving the ATRA products **4da–4do** in good to high yield, comparing favorably to iridium catalysts[7] (Scheme 3D). Late-stage functionalization of more complex, biologically relevant molecules delivered the corresponding 1,3-functionalized products **4ea–4ef** in 61–95 % yield (Scheme 3E). Scale-up was demonstrated for **4a** (10 mmol, 2.17 g, 89 %), employing readily available and inexpensive $[Cu(dmp)_2Cl]$ in a simple batch setup requiring a slightly prolonged reaction time (5 h, Scheme 4A).

The obtained ATRA products show attractive synthetic utility, and especially the bromide functionality offers manifold possibilities for subsequent transformations with oxygen, nitrogen, sulfur, or carbon-based nucleophiles leading to nitro derivatives **5a–5f** (Scheme 4A). It should be

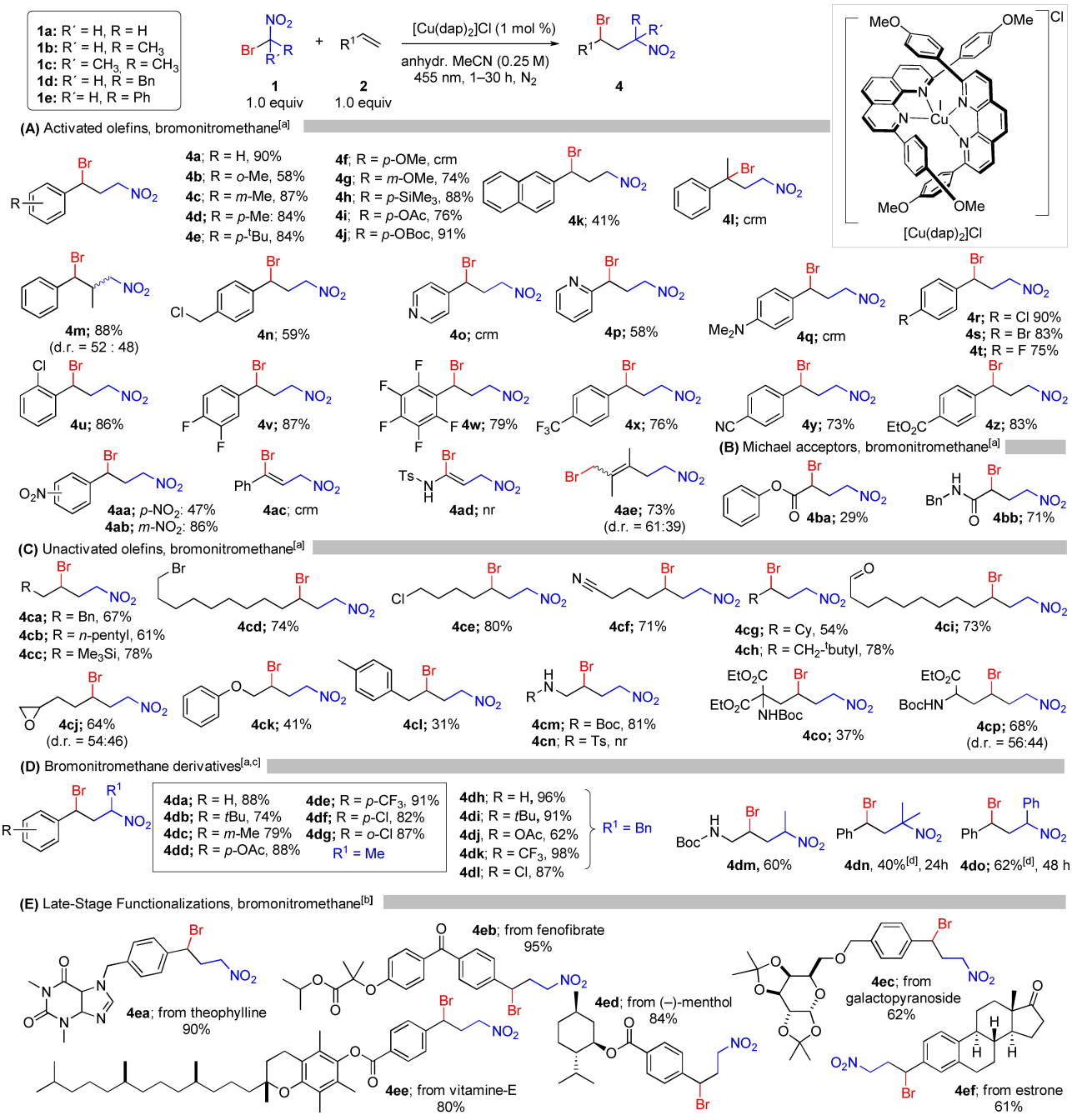

Scheme 3. Substrate scope [a] 0.5 mmol scale in MeCN [b] 0.5 mmol scale in solvent mixtures (MeCN/DCM/$CHCl_3$; see Supporting Information for details). [c] d.r. 1 : 1–2 : 1 [d] ^{1}H NMR yield using 1,3,5-trimethoxybenzene as internal standard. crm = complex reaction mixture, nr = no reaction. Isolated yields are given unless otherwise stated.

noted that in many ATRA processes such as in the chlorosulfonylation,[10] the 1,2-placement of the functional groups at the alkene only allows elaboration of the halide in a limited way since rapid dehydrohalogenation generally takes place. In the current methodology, the functional groups are placed in a 1,3-relationship, thus opening different reactivity pathways. This is highlighted by the transformation of the bromo and nitro functionality to the corresponding nitroalkane **6a** or the amine **6b** (Scheme 4B). Given the value of amino cyclopropanes as a structural motif in several bioactive compounds,[15] we investigated their formation from representative 1,3-bromonitroproducts **4** in the presence of a base (Scheme 4C). Thus, **4v** can be in converted in the corresponding aminocyclopropane,[16] which is required to construct ticagrelor (**8v**), an important platelet aggregation inhibitor.[17]

Estrone derivative **4ef** can be used to synthesize the highly substituted nitrocyclopropane **7ef**, while, according to a literature report,[20] histone demethylase LSD1 inhibitor **8j** can be obtained from nitrocyclopropane **7j**. Noteworthy, the

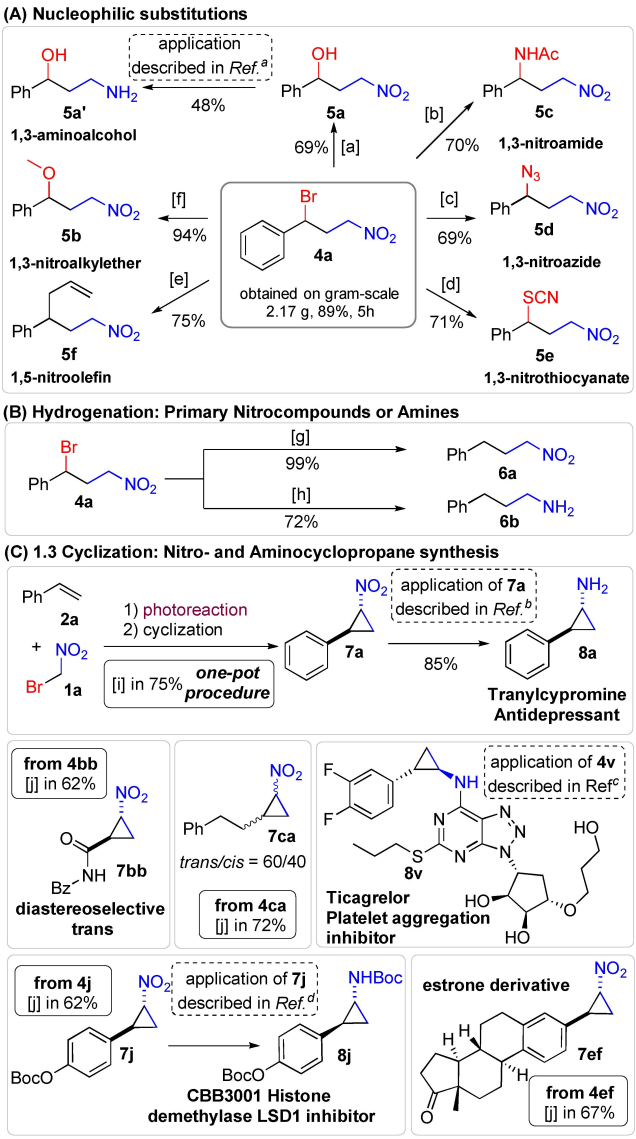

Scheme 4. Synthetic Utility (0.5 mmol scale): [a] acetone/water (1:1), 2 h, reflux. [b] $FeCl_3 \cdot 6\,H_2O$ (4.0 equiv), MeCN, 2 h, 80 °C. [c] NaN_3 (5.0 equiv), DMF, 2 h, 25 °C. [d] NaSCN (5.0 equiv), DMF, 2 h, 25 °C. [e] allyltrimethylsilane (2.0 equiv), $FeCl_3$ (5 mol%), DCM, 2 h,25 °C. [f] MeOH, 2 h, 65 °C. [g] MeOH, Pd/C (10 mol%) H_2 (1 atm), 22 h, 25 °C. [h] 0.8 mmol scale, Zn (24 equiv), aqueous AcOH, 18 h, 25 °C. [i] Cu-photocatalyzed ATRA reaction of **1a** with **2a** (conditions, see Scheme 3), followed by addition of DBU (2.0 equiv) to the reaction mixture, 30 min, 25 °C. [j] ATRA product, DBU (2.0 equiv), THF, 30 min, 25 °C. Ref.[a].[18] Ref.[b].[19] Ref.[c].[16] Ref.[d].[20]

direct addition of DBU to the reaction mixture of the ATRA reaction, exemplified for **4a**, leads in a one-flask protocol to nitrocyclopropane **7a**, which can be further converted[19] to the monoamine oxidase inhibitor tranylcypromine (**8a**).[21]

Further mechanistic details revolving around the postulated key steps and intermediates under the Cu^{I} catalysis in direct comparison to Ooi's Ir^{III}-catalysis were studied by CW-EPR spectroscopy (X-band). Especially the experimental identification of postulated persistent radical **C** (R = Bn) that was predicted by Ooi et al. based on DFT calculations[7] was addressed: Based on the redox potentials of the respective catalysts and the unique ability of ligand exchange of copper, it was concluded that the contrary product selectivity of the Cu- vs. $Ir(ppy)_3$-catalysis are closely linked to the presence (Ir) or absence (Cu) of the radical **C**. Indeed, if $Ir(ppy)_3$ was employed as a photocatalyst in presence of **1a**, **1b**, **1d** and styrene (**2a**), the formation of an organic radical ($g_{iso} = 2.006$) was observed, whereas no organic radical could be detected in the [Cu^{I}-$(dap)_2$]Cl catalyzed reaction (Scheme 5B) (see Supporting Information). The EPR signal under Ir-catalysis grew steadily over a period of more than 15 min indicating its persistent character as an intermediate, quite similar to related nitronic ester radicals.[22]

The observed typical triplet signature of a nitrogen-centered radical showed with a g-value of 2.006 and α_N of 1.4 mT comparable parameters to TEMPO ($\alpha_N = 1.6$ mT) and related nitronic ester radicals[22] (see Supporting Information for details). Based on the triplet signature of the EPR signal the acyclic carbon centered radical **B** was excluded to be the cause of this signal. In addition, radical **A** formed via the mesolytic cleavage of the carbon-bromine bond of the radical anion of **1**, was likewise excluded by

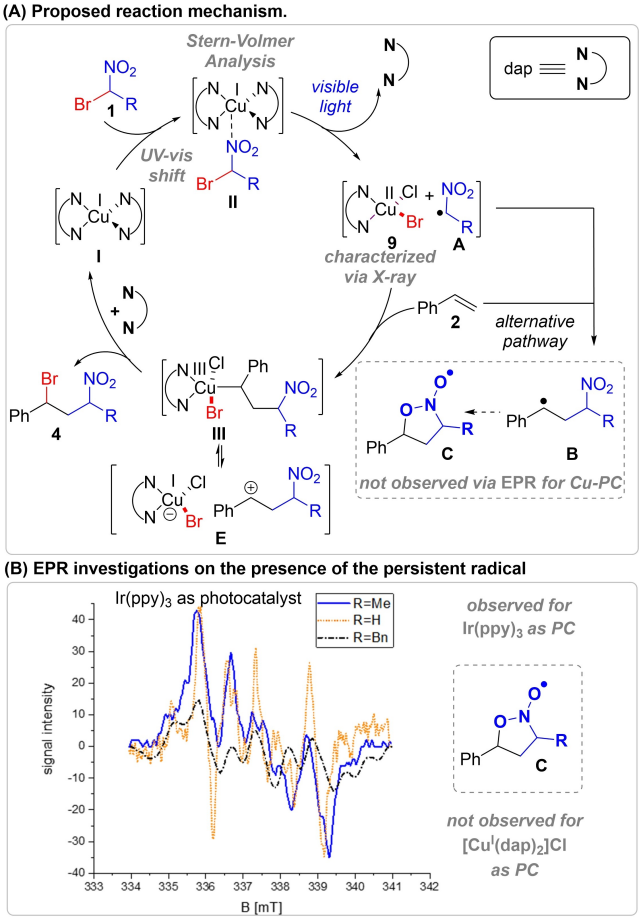

Scheme 5. (A) Proposed reaction mechanism; (B) mechanistic studies: (for detailed experimental conditions, see Supporting Information).

three reasons: its expected short lifetime, the different splitting pattern, and the fact, that the observed EPR signal shown in Scheme 5 only occurs in the presence of styrene (**2a**). Under tuned measurement conditions the anisotropy in the hyperfine splitting and g-values as well as the coupling to the α-H-atoms of the nitronic-ester radicals could be partially resolved (Scheme 5B).

A plausible reaction mechanism (Scheme 5A) therefore begins with the coordination of ATRA reagent **1** to the photocatalyst **I** as indicated by UV/Vis absorption shifts of the binary mixture of photocatalyst $[Cu^{I}(dap)_2]Cl$ and **1** prior to irradiation (see Supporting Information). Single electron transfer from **II** to ATRA reagent **1** and subsequent cleavage of the C–Br bond yields intermediate **9** and radical **A**. Stern-Volmer studies support this step by showing quenching of the exited state of the photocatalyst $[Cu^{I}(dap)_2]Cl$ by **1a** only, but not by styrene (**2a**) (see Supporting Information). Further support of this oxidation step was found by X-ray analysis[23] of single crystals obtained from a solution of $[Cu^{I}(dap)_2]Cl$ in the presence of **1a** having the molecular structure $[Cu^{II}(dap)ClBr]$ (**9**) (see Supporting Information). "In situ" evidence of this redox-change was provided by EPR measurements of an equimolar solution of $[Cu^{I}(dap)_2]Cl$ and **1b** in MeCN, which delivered a typical Cu^{II} spectrum indicating an octahedral coordination with an axial elongation of the ligands (see Supporting Information). This Cu^{II} species was even observable if 10 mol % $[Cu^{I}(dap)_2]Cl$ were employed, suggesting that this step happens with high probability also under catalytic conditions. To test for the onward elementary steps, 1 equiv of styrene (**2a**) was added to this binary mixture after confirming the Cu^{II} species. The intensity of the Cu^{II} signal was immediately reduced indicating a quick turn over to a diamagnetic Cu-species. Also, even under such high catalyst loadings no EPR-signature of **C** was observed.

Since no organic radical could be detected in the EPR studies of the Cu-catalyzed reaction, we deduce from our experiments that Cu^{II} modulates the radical reactivity by the formation of a (formal) Cu^{III}-intermediate[24–26] **III** (or ion pair **E** representing the direct oxidation of radical **B**) so that the cyclization pathway to radical **C** is not competitive anymore (see above, Scheme 5). An alternative interpretation for the absence of the EPR-signal of **C**, would be a quick turnover of **C** in the presence of Cu^{II}. This was ruled out based on the associated redox-potentials and additional EPR experiments (see Supporting Information), which showed that **C** is not quenched by Cu^{II}.

In conclusion, we have developed a highly efficient Cu^{I}-photocatalyzed visible light-mediated ATRA reaction of bromonitromethane derivatives and olefins. Besides the synthetic value of the title reaction concerning scope and further transformations of the products, we present evidence for the highly efficient rebound of Cu^{II} to radical intermediates that can even outcompete a favorable intramolecular cyclization to a persistent radical. It is acknowledged that the ultimate proof of the mechanistic proposal would be the isolation of a Cu^{III}-intermediate along the reaction pathway, which represents a great challenge[24–26] given the rapid reductive elimination that can take place to yield the ATRA product with concurrent regeneration of the Cu^{I}-photocatalyst.

Acknowledgements

This work was supported by the Fonds der Chemischen Industrie (fellowship to A. R.) and the DFG—TRR 325444632635-A1 (M. K.), RE3630/5 (H. S.), and RE948/18 (A. R.). We thank B. Eichenseher and P. Kreitmeier for the synthesis of starting materials, J. Kiermaier and W. Söllner for Mass analysis and Dr. M. Bodensteiner, S. Stempfhuber and B. Hischa for X-Ray analyses (all University of Regensburg). Open Access funding enabled and organized by Projekt DEAL.

Conflict of Interest

The authors declare no conflict of interest.

Data Availability Statement

The data that support the findings of this study are available in the supplementary material of this article.

Keywords: Copper · Homogeneous Catalysis · Photocatalysis · Radicals · Reaction Mechanism

[1] a) M. S. Kharasch, E. V. Jensen, W. H. Urry, *Science* **1945**, *102*, 128; b) M. S. Kharasch, W. H. Urry, E. V. Jensen, *J. Am. Chem. Soc.* **1945**, *67*, 1626; c) M. S. Kharasch, P. S. Skell, P. Fisher, *J. Am. Chem. Soc.* **1948**, *70*, 1055.
[2] M. H. Shaw, J. Twilton, D. W. C. MacMillan, *J. Org. Chem.* **2016**, *81*, 6898.
[3] T. Courant, G. Masson, *J. Org. Chem.* **2016**, *81*, 6945.
[4] A. Hossain, A. Bhattacharyya, O. Reiser, *Science* **2019**, *364*, aav9713.
[5] S. Engl, O. Reiser, *Chem. Soc. Rev.* **2022**, *51*, 5287.
[6] a) H. Cao, S. Ma, Y. Feng, Y. Guo, P. Jiao, *Chem. Commun.* **2022**, *58*, 1780; b) G. Hirata, T. Shimada, T. Nishikata, *Org. Lett.* **2020**, *22*, 8952; c) M. Iwasaki, Y. Ikemoto, Y. Nishihara, *Org. Lett.* **2020**, *22*, 7577.
[7] Y. Tsuchiya, R. Onai, D. Uraguchi, T. Ooi, *Chem. Commun.* **2020**, *56*, 11014.
[8] a) S. Engl, O. Reiser, *Eur. J. Org. Chem.* **2020**, 1523; b) C. K. Prier, D. A. Rankic, D. W. C. MacMillan, *Chem. Rev.* **2013**, *113*, 5322.
[9] M. P. Thorpe, A. N. Smith, M. S. Crocker, J. N. Johnston, *J. Org. Chem.* **2022**, *87*, 5451–5455.
[10] A. Hossain, S. Engl, E. Lutsker, O. Reiser, *ACS Catal.* **2019**, *9*, 1103.
[11] C. Minozzi, A. Caron, J.-C. Grenier-Petel, J. Santandrea, S. K. Collins, *Angew. Chem. Int. Ed.* **2018**, *57*, 5477; *Angew. Chem.* **2018**, *130*, 5575.
[12] S. Engl, O. Reiser, *ACS Catal.* **2020**, *10*, 9899.
[13] S. Paria, M. Pirtsch, V. Kais, O. Reiser, *Synthesis* **2013**, *45*, 2689.

[14] X.-J. Tang, W. R. Dolbier, *Angew. Chem. Int. Ed.* **2015**, *54*, 4246; *Angew. Chem.* **2015**, *127*, 4320.
[15] a) T. Akasaka, S. Kurosaka, Y. Uchida, M. Tanaka, K. Sato, I. Hayakawa, *Antimicrob. Agents Chemother.* **1998**, *42*, 1284; b) S. Kawamura, Y. Unno, A. List, A. Mizuno, M. Tanaka, T. Sasaki, M. Arisawa, A. Asai, M. Groll, S. Shuto, *J. Med. Chem.* **2013**, *56*, 3689; c) H.-L. Teng, Y. Luo, B. Wang, L. Zhang, M. Nishiura, Z. Hou, *Angew. Chem. Int. Ed.* **2016**, *55*, 15406; *Angew. Chem.* **2016**, *128*, 15632.
[16] K. G. Hugentobler, H. Sharif, M. Rasparini, R. S. Heath, N. J. Turner, *Org. Biomol. Chem.* **2016**, *14*, 8064.
[17] M. Rasparini, M. Taddei, E. Cini, C. Minelli, N. Turner, K. G. Hugentobler, Rasparini, Marcello; Taddei, Maurizio; Cini, Elena; Minelli, Cosima; Turner, Nicholas; Hugentobler, Katharina, A1 2013-05-08, **2013**.
[18] S. Tanaka, S. Kohmoto, M. Yamamoto, K. Yamada, *Nippon Shokuhin Kagaku Kogaku Kaishi* **1989**, 1742.
[19] B. Moreau, D. Alberico, V. N. Lindsay, A. B. Charette, *Tetrahedron* **2012**, *68*, 3487.
[20] N. Hoang, X. Zhang, C. Zhang, V. Vo, F. Leng, L. Saxena, F. Yin, F. Lu, G. Zheng, P. Bhowmik, et al., *Bioorg. Med. Chem.* **2018**, *26*, 1523.
[21] S. Ulrich, R. Ricken, M. Adli, *Eur. Neuropsychopharmacol.* **2017**, *27*, 697.
[22] J. E. T. Corrie, B. C. Gilbert, V. R. N. Munasinghe, A. C. Whitwood, *J. Chem. Soc. Perkin Trans. 2* **2000**, 2483.
[23] Deposition numbers 2192294 (**4h**) and 2192295 (**9**) contain the supplementary crystallographic data for this paper. These data are provided free of charge by the joint Cambridge Crystallographic Data Centre and Fachinformationszentrum Karlsruhe Access Structures service.
[24] L. M. Huffman, S. S. Stahl, *J. Am. Chem. Soc.* **2008**, *130*, 9196.
[25] A. E. King, L. M. Huffman, A. Casitas, M. Costas, X. Ribas, S. S. Stahl, *J. Am. Chem. Soc.* **2010**, *132*, 12068.
[26] L. M. Huffman, A. Casitas, M. Font, M. Canta, M. Costas, X. Ribas, S. S. Stahl, *Chem. Eur. J.* **2011**, *17*, 10643.

Manuscript received: December 25, 2022
Accepted manuscript online: February 2, 2023
Version of record online: March 8, 2023